Geomechanics and Engineering, *Vol. 36, No. 2 (2024) 157-166*
https://doi.org/10.12989/gae.2024.36.2.157

Acceleration amplification characteristics of embankment reinforced with rubble mound

Jung-Won Yun[1], Jin-Tae Han*[2] and Jae-Kwang Ahn[3]

[1]*Department of Civil Engineering, Korea Army Academy at Yeongcheon, Yeongcheon, South Korea*
[2]*Department of Geotechnical Engineering Research, Korea Institute of Civil Engineering and Building Technology, Gyeonggi, South Korea*
[3]*Earthquake and Volcano Technology Team, Korea Meteorological Administration, Seoul, South Korea*

(*Received October 4, 2023, Revised December 24, 2023, Accepted December 26, 2023*)

Abstract. Generally, the rubble mound installed on the slope embankment of the open-type wharf is designed based on the impact of wave force, with no consideration for the impact of seismic force. Therefore, in this study, dynamic centrifuge model test results were analyzed to examine the acceleration amplification of embankment reinforced with rubble mound under seismic conditions. The experimental results show that when rubble mounds were installed on the ground surface of the embankment, acceleration response of embankment decreased by approximately 22%, and imbalance in ground settlement decreased significantly from eight to two times. Furthermore, based on the experimental results, one-dimensional site response (1DSR) analyses were conducted. The analysis results indicated that reinforcing the embankment with rubble mound can decrease the peak ground acceleration (PGA) and short period response (below 0.6 seconds) of the ground surface by approximately 28%. However, no significant impact on the long period response (above 0.6 seconds) was observed. Additionally, in ground with lower relative density, a significant decrease in response and wide range of reduced periods were observed. Considering that the reduced short period range corresponds to the critical periods in the design response spectrum, reinforcing the loose ground with rubble mound can effectively decrease the acceleration response of the ground surface.

Keywords: acceleration amplification; centrifuge model test; embankment; one-dimension site response analysis; rubble mound

1. Introduction

A wharf is a type of coastal structure installed along the coast of berth vessels and is classified into closed and open types. A closed-type wharf is constructed by vertically erecting a front wall and filling it with materials such as soil or concrete during construction. However, an open-type wharf is a form in which water flows beneath a deck constructed on piles (Balomenos and Padgett 2018). The slope embankment of an open-type wharf can be exposed to wave forces; therefore, protective materials are installed on the embankment to protect the internal components (McCullough *et al.* 2007, Su *et al.* 2017, Vytiniotis *et al.* 2019). For an embankment material exposed to wave forces, a stable mass should be secured to prevent disruption of the material, and the mass should be calculated using either physical model experiments or the Hudson formula suitable for the given conditions (Hudson 1959, MOF 2017).

The design criteria for the embankment material of an open-type wharf typically consider the effects of wave forces rather than those of seismic forces (PIANC 2001, MOF 2017). Generally, the purpose of constructing open-type wharves is to prevent the collapse of embankments owing to wave forces. However, attention should be paid to the vulnerability of coastal embankments constructed with loose sediments to seismic events (Lee *et al.* 2007). Therefore, various experimental and numerical studies have been conducted to examine the relationship between the seismic forces and rubble mounds used as cladding materials (Memos *et al.* 2001, Cihan and Yuksel 2011, Ye and Jeng 2013, Ye and Wang 2015, Najma and Ghalandarzadeh 2019). Memos *et al*. (2001) conducted 1 g shaking-table tests to investigate the seismic behavior of a breakwater embankment reinforced with rubble mounds.

The experiments revealed that seismic performance was secured when there was dense ground inside the rubble mound; however, significant residual displacement was noted in cases where loose ground existed. Cihan and Yuksel (2011) conducted shaking table tests to examine the seismic behavior of a breakwater embankment reinforced with rubble mounds, with and without substructure elements (toes). They compared the experimental results with numerical analysis and found that the slope stability of the embankment increased when substructure elements (toes) were placed at both ends of the embankment to prevent the lateral spread of the structure. Najma and Ghalandarzadeh (2019) performed 1 g shaking table tests to evaluate the dynamic behavior of caisson and rubble mound breakwaters during soil liquefaction. In addition, some researchers conducted numerical studies to investigate the stability of rubble mounds during seismic events (Ye and Jeng 2013, Ye and Wang 2015).

*Corresponding author, Ph.D.
E-mail: jimmyhan@kict.re.kr

ISSN: 2005-307X (Print), 2092-6219 (Online)

As aforementioned, studies on the stability of breakwater embankments with rubble mounds during seismic events have been conducted, focusing primarily on analyzing the displacement patterns of embankments. Therefore, Yun and Han (2023a) conducted centrifuge model tests to analyze the acceleration response of the ground and– soil-pile interactions with and without rubble mounds. However, in their study, the tests were conducted based on a single acceleration time history, and they did not consider the various seismic motions that change over time. Generally, even when the same magnitude of seismic parameters (i.e., peak ground acceleration (PGA), peak ground velocity (PGV), and peak ground displacement (PGD)) is applied to a slope, differences in the displacement response can occur depending on the characteristics of the seismic motion (Lee *et al.* 2015). Hence, a comprehensive assessment that considers various seismic motion characteristics is necessary to evaluate the dynamic response of the ground with and without rubble mounds.

In this study, the dynamic responses of embankments reinforced with rubble mounds were analyzed based on the results of dynamic centrifuge model tests conducted by Yun and Han (2023a). Additionally, one-dimensional site response analyses (1DSR) were performed using the properties applied in the experiments. The 140 model cases were considered for the analyses, and the amplification characteristics of the ground reinforced with rubble were analyzed using the obtained results.

In this study, 1DSR analyses were performed based on centrifuge model test that accounted for slope geometry, thereby imposing constraints and limitations on the comparative validation for two-dimensional problems.

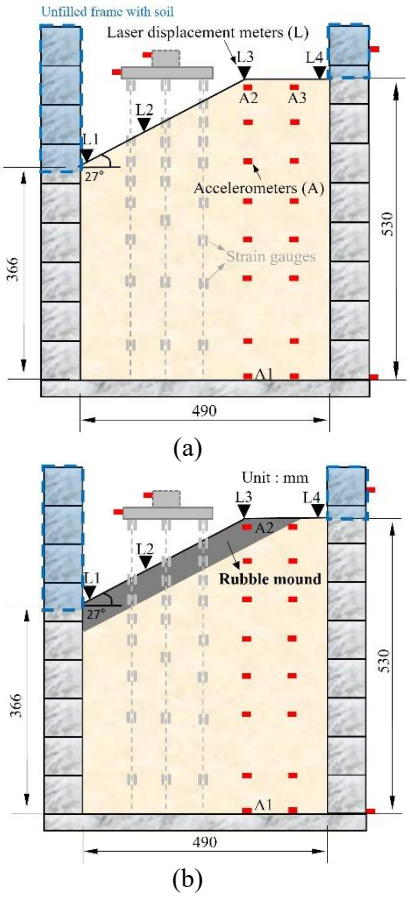

Fig. 1Model cross-section (Yun and Han 2023a); (a) NRM model and (b) CRM model (in model scale, unit: mm)

2. Centrifuge model test

A centrifuge model test replicates the actual stress in the ground by magnifying the gravitational acceleration n times in a model scaled down by a factor of $1/n$ (Lees and Richards 2011, Yun *et al*. 2022, Yun *et al*. 2023b). where n denotes the scale factor. The experimental model proposed by Yun and Han (2023a) was used in this study. The experimental model was defined as non-covered with rubble mound (NRM) and covered with rubble mound (CRM) based on the presence or absence of the rubble mound, as shown in Fig. 1. Following the scaling law in Table 1, reduced-scale models were fabricated, and experiments were conducted at a centrifugal acceleration of 34 g. Additionally, dry silica sand was used in the experiments to achieve a relative density of 50% after air-pluvation. The material properties of the soil are summarized in Table 2. The rubble mounds installed on the upper slope of the embankment were manufactured by rapid filtration of Jumunjin soil in Korea by reducing the size of commonly used particles (100–500 mm) to a 1/34 scale (Fig. 2). The material properties of the rubble mounds are listed in Table 3.

The input seismic motions used in the experiment were produced by matching the Masan Observatory data of the Gyeongju earthquake that occurred in Korea in 2016 with

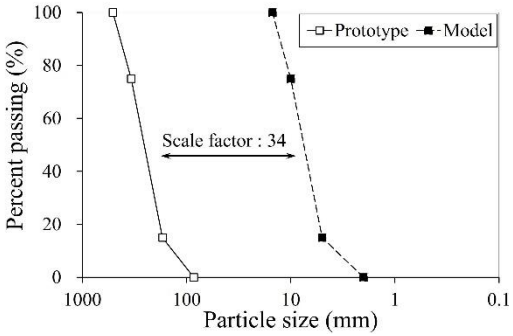

Fig. 2 Rock gradations used in the models (Yun and Han 2023a)

the design response spectrum. Spectrum matching finely adjusts the period and amplitude of the actual seismic motion to match the target response period (Al Atik and Abrahamson 2010). In this study, the target design response spectrum was established using the S1 soil conditions (bedrock) as defined in the "Announcement of common application of seismic design criteria" by the Ministry of Land, Infrastructure and Transport of Korea (MOIS 2017).

The amplitude of the earthquake applied a value ranging from 0.07 to 0.22 g based on the PGA. Fig. 3(a) shows the result of normalizing the peak ground acceleration of the

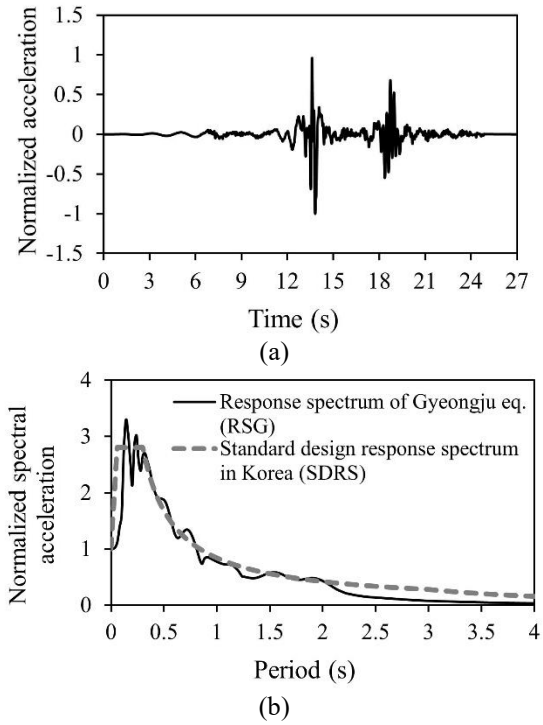

Fig. 3 Normalized time history curve and response spectrum curve: (a) time history of Gyeongju earthquake and (b) response spectrum curve

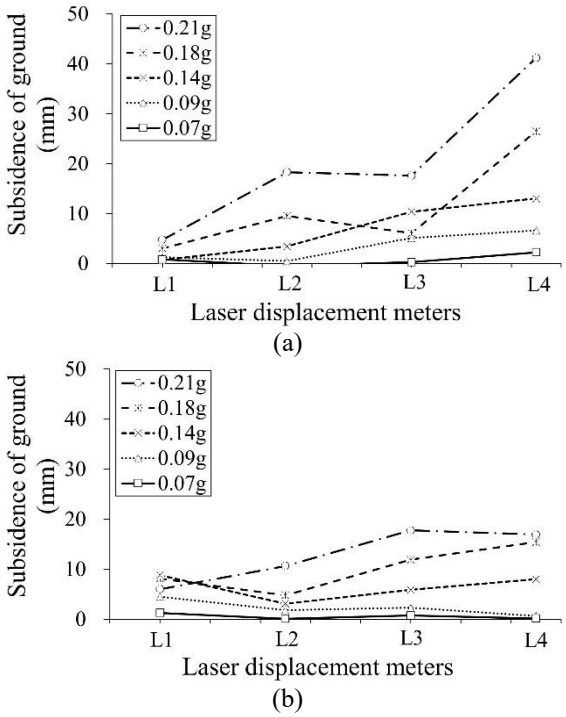

Fig. 4 Ground subsidence of NRM and CRM models: (a) NRM model and (b) CRM model (in prototype scale)

Table 1 Prototype and model properties

Quantity	Model/ Prototype	Quantity	Model/ Prototype
Stress, modulus	1	Force, load	N^{-2}
Density	1	Mass	N^{-3}
Lenth, displacement	N^{-1}	Diffusion time	N^{-2}
Gravity	N	Stress wave velocity	1
Strain	1	Dynamic acceleration	N

Table 2 Basic properties of the silica sand used in the experiments

Soil property	USCS	C_c	C_u	G_s	$\gamma_{d.max}$ (kN·m^{-3})	$\gamma_{d.min}$ (kN·m^{-3})
Silica sand	SP	1.16	1.96	2.63	16.5	12.4

Table 3 Basic properties of the rubble mound used in the experiments

c	USCS	C_c	C_u	G_s	$\gamma_{d.max}$ (kN·m^{-3})	$\gamma_{d.min}$ (kN·m^{-3})
Rubble mound	GP	1.09	2.2	2.65	17.7	16.2

time history curve to 1, and Fig. 3(b) shows the result of normalizing the peak ground acceleration (at period = 0) of the response spectrum curve to 1.

When deformation occurs in the embankment of an open-type wharf, the active force of the ground exerts additional effects on the foundation. Hence, the MOF (1999) proposed design criteria based on the allowable displacements of embankments, with displacement limits of 10 and 30 cm for functional performance and collapse prevention, respectively. Similarly, PINAC (2001) proposed subsidence criteria of 10 and 30 cm based on performance levels, considering the differential settlement between the backfill soil and the upper part of the structure. Consequently, in this study, ground subsidence with and without a rubble mound was compared to evaluate the performance of an embankment with a rubble mound.

Fig. 4 presents the ground subsidence results of the NRM and CRM models, along with the results converted to the prototype scale. The horizontal axis of each model represents the position of the laser displacement sensor, and the vertical axis indicates the ground subsidence. Cumulative subsidence after five earthquake events for each model is shown. Based on the graph, when the input acceleration is below 0.14 g, the difference in ground subsidence with and without the rubble mound is not significant. However, at input acceleration of 0.18 and 0.21 g, the difference in ground subsidence increases significantly. Particularly, at an input acceleration of 0.21 g, the NRM model exhibits cumulative subsidence of over 40 mm at location L4, while experiencing approximately 5 mm of subsidence at location L1. This approximately 8-fold difference in subsidence between the lower and upper ground positions indicates an uneven distribution of ground subsidence around the embankment during an earthquake. However, under an input acceleration of 0.21 g, the CRM model shows a cumulative subsidence of 20 mm at location L4 and 10 mm at location L1. The difference in subsidence between the lower and upper portions was less than 2-fold, indicating a reduced imbalance in ground subsidence compared with the NRM model.

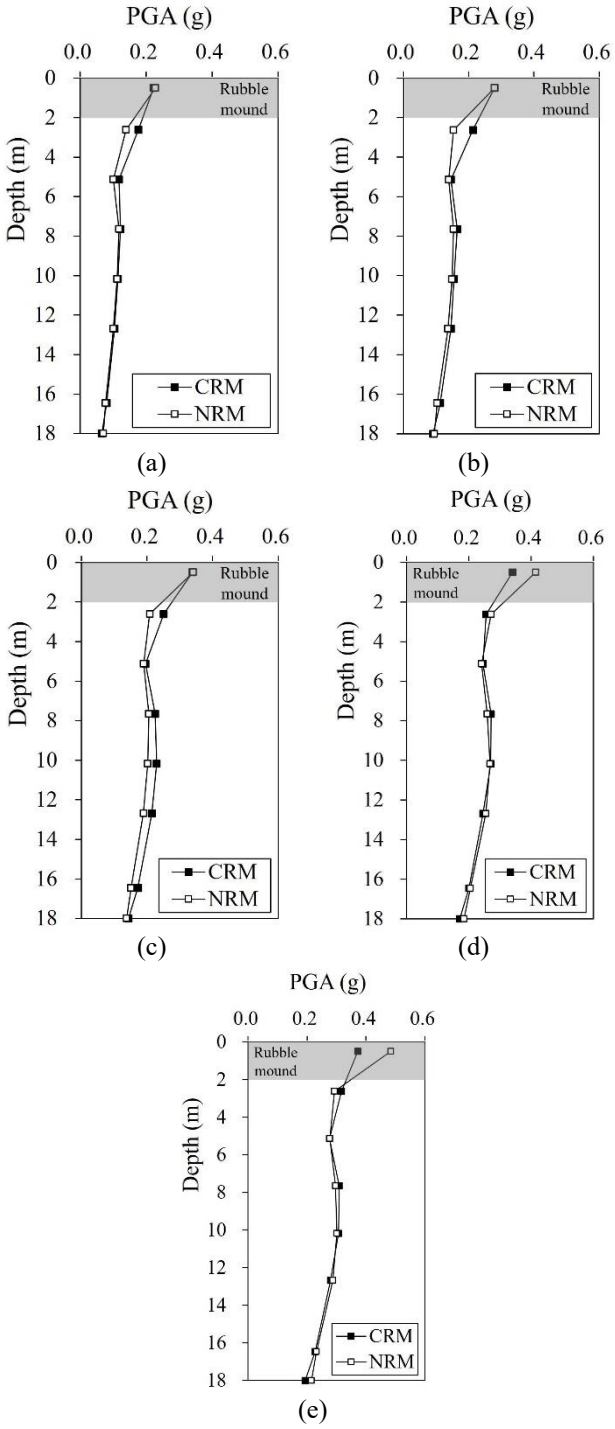

Fig. 5 Centrifuge results of PGA along the depth: (a) 0.07 g, (b) 0.09 g, (c) 0.14 g, (d) 0.18 g and (e) 0.21 g (in prototype scale)

Fig. 5 shows the acceleration results for the NRM and CRM models. Each figure illustrates the depth-based PGA derived from the accelerometers positioned beneath the accelerometer (A2) located at the top of the embankment. These figures show the responses based on the amplitude of the input acceleration. First, when input accelerations are below 0.14 g, the ground surface PGA between the NRM and CRM models appears similar. However, under input acceleration of 0.18 and 0.21 g, the ground surface PGAs were found to be 16 and 22% smaller in the CRM model compared to the NRM model. This indicates a significant difference in ground deformation depending on the rubble mound as the input acceleration increases. As shown in Fig. 4, the ground stiffness decreased and the ground acceleration response increased as the ground surface of the NRM experimental model was disturbed.

In summary, the experimental results indicate that in the CRM model, compared with the NRM model, the acceleration response at the ground surface of the embankment decreased by approximately 22%, and ground subsidence decreased by approximately 50%. Moreover, the imbalance in subsidence between the lower and upper ground positions decreased significantly from 8-fold to 2-fold. Therefore, it can be inferred that installing a rubble mound on an embankment enhances the seismic performance in terms of both acceleration and displacement.

3. One-dimensional site response (1DSR) analysis

3.1 1DSR analysis model and verification

As aforementioned, to evaluate the dynamic response of ground with a rubble mound, a comprehensive assessment considering various seismic motion characteristics is required. To address this issue, one-dimensional site response (1DSR) analyses were conducted using multiple seismic motions. The 1DSR is a frequency-domain analysis method that indirectly considers the nonlinear behavior of soil based on shear deformation. For 1DSR analysis, the Proshake software (version 2.0) was used (EduPro Civil System, Inc., 2017).

In this section, the dynamic properties of the soil were determined for application in the 1DSR analysis. First, the shear wave velocity based on the ground confining pressure was calculated from the resonant column test results. The resonant column test is a method in which torsional vibrations of varying frequencies are applied to a cylindrical soil specimen to determine the resonant frequency and amplitude of vibration in the first model and then derive the dynamic properties of the ground. Fig. 6 presents the resonant column test results of 55% relative density ground, similar to this experimental model, and the results of 80% relative density ground. The shear wave velocities corresponding to different confining pressures were measured using a resonant column test. The input properties for the analysis were determined based on the measured data. In the case of the input properties, the stratum was divided into 1 m intervals, and the shear wave velocity based on the confining pressure of each stratum was calculated.

Subsequently, soil models were selected to simulate the shear deformation and damping characteristics of the ground. Typically, models developed by Seed and Idriss (1970) and Darendeli (2001) have been widely applied to simulate sand layers. Seed and Idriss (1970) developed a sand model that provides applicable values for shear

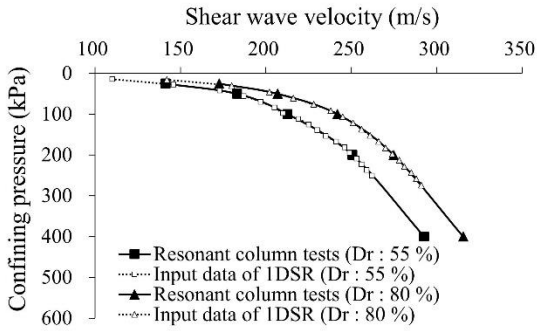

Fig. 6 Resonant column test results and input data of 1DSR analysis

Table 4 Analysis conditions

Relative density	Analysis model	Input motion	Recurrence periods (amplitude)
55% 80%	NRM model CRM model	Gyeongju (Korea) Pohang (Korea) Borah Peak-PBF (U.S.A) Nahanni-Nahanni (Canada) Romania-Istrita (Romania) Tabas-dayhook (Iran) Tabas-Tabas (Iran)	100 years (0.063 g) 200 years (0.08 g) 500 years (0.11 g) 1000 years (0.154 g) 2400 years (0.22 g)

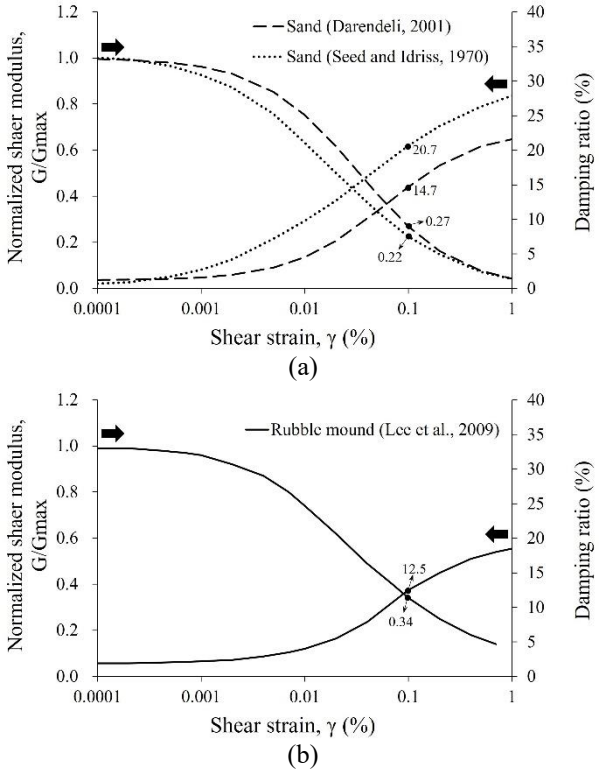

Fig. 7 Normalized shear modulus and damping ratio (confining pressure: 140 kPa, 10 m depth): (a) sand model and (b) rubble mound model

modulus (G_{max}) and damping ratio. The model provides upper-bound values for the shear modulus curve and lower-bound values for the damping curve. Later, Darendeli (2001) proposed a model that encompasses a wide range of soil properties, which researchers established by supplementing existing experimental data with additional resonant column and torsional shear tests. The modified model demonstrated its capability to appropriately simulate experimental results. Fig. 7(a) compares the normalized shear modulus (G/G_{max}) and damping ratio curves of the soil obtained using the Seed and Idriss (1970) and Darendeli (2001) models. The figure shows the results under confining-pressure conditions at a ground depth of approximately 10 m. It can be observed that G/G_{max} is smaller in the Seed and Idriss (1970) than in the Darendeli (2001) models, and the damping ratio is significantly higher. This is consistent with the findings of Dammala *et al.* (2017). Dammala *et al.* (2017) performed multiple resonant column tests under three confining pressure conditions (50, 100, and 300 kPa) using sand collected from rivers near the Himalayan mountains, where earthquakes occur frequently. In their study, 1DSR analyses were performed along with the shear modulus and damping curve of the ground model, including Seed and Idriss (1970) and Darendeli (2001), to compare the acceleration by depth. The results of the comparison indicated that the Seed and Idriss (1970) model tended to underestimate the normalized shear modulus, overestimate the damping ratio, and consequently underestimate the ground acceleration when compared to the Darendeli (2001) model. Therefore, in this study, analyses were performed using Darendeli's (2001) model to simulate the sand layer.

For the rubble mound, the model derived by Lee *et al.* (2009) was applied. Lee *et al.* (2009) established a database for rubble materials based on 18 papers published from 1988 to 2006 in the United States and Japan to evaluate the nonlinear dynamic deformation characteristics of the rockfill zone materials of dams. Generally, a specimen for a large-scale triaxial test is 300 mm in diameter and 600 mm in height; therefore, it is impossible to perform the test while satisfying the conditions of the actual component materials. Therefore, testing was performed by adjusting the particle size of the sample to be suitable for the sample size. The maximum particle size of the test sample in the above studies was 303 mm. In their study, 135 normalized shear modulus curves and 65 damping ratio curves were obtained. The representative curves were selected based on these results. Fig. 7(b) shows a comparison of the normalized shear modulus (G/G_{max}) and damping ratio curves of the ground to which the rubble mound model derived by Lee *et al.* (2009) was applied.

For the input seismic motion used in the analysis, five types of intraplate earthquakes (Borah, Nahanni, Romania, Tabas-Dayhook, and Tabas-Tabas) were selected with the Gyeongju and Pohang earthquakes that occurred in Korea. It was manufactured by matching the acceleration spectrum with the response spectrum curve considering the ground characteristics. Fig. 8 shows the acceleration time-history curves for each seismic motion. The Gyeongju earthquake exhibited the same motion as that used in the experiments.

For other seismic motions, data provided by the Korea Authority of Land and Infrastructure Safety (KALIS) were

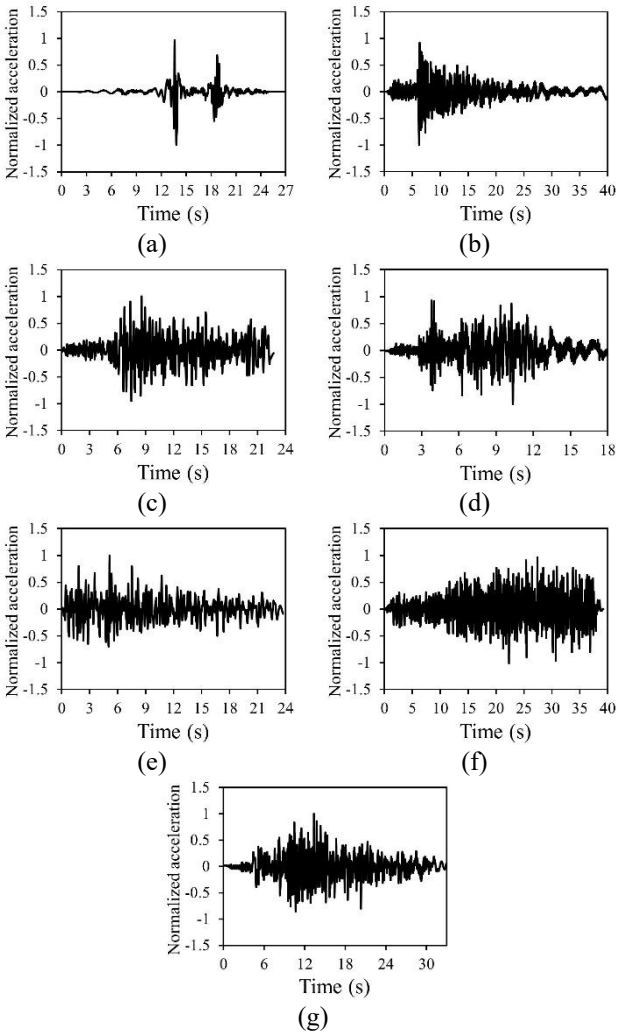

Fig. 8 Normalized time history of input earthquake: (a) Gyeongju, (b) Pohnag, (c) Borah, (d) Nahanni, (e) Romania, (f) Tabas-Dayhook and (g) Tabas-Tabas seismic motion

used. The selected seismic motions were scaled to correspond to the average recurrence periods of 100, 200, 500, 1,000, and 2,400 years. The amplitudes were determined as 0.063, 0.08, 0.11, 0.154, and 0.22 g, respectively. A total of 140 analyses were conducted in this study, considering two relative densities: the presence of a rubble mound, seven different input earthquake motions, and five amplitude levels. The analytical conditions are listed in Table 4.

Fig. 9 compares the PGA based on the depth and response spectra of the ground surface derived from the experiment and analysis to verify the 1DSR analysis model. For comparison, the CRM model was selected with an input acceleration of 0.07 g, where ground settlement was minimal. The experimental and analysis models subjected to the Gyeongju seismic motions are shown as solid and dotted black lines, respectively, whereas the analysis models for the other six seismic motions are shown as solid gray lines. The figure shows that the analysis model adequately simulates the depth-dependent PGA values of

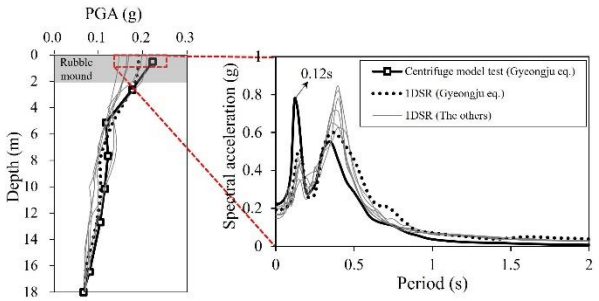

Fig. 9 Comparison of PGA of experimental and 1DSR analysis model (CRM model, input base acceleration: 0.07 g, in prototype scale)

the experimental model. However, the upper PGA was derived as 0.22 g in the experimental model, it ranged from 0.15 to 0.21 g in the analysis models, indicating a somewhat larger response in the experimental model. This was attributed to the substantial contribution of the short period component in the experimental model. Based on the response spectrum curves in Fig. 9, the response around 0.12 s was extremely large in the experimental model compared to the analysis model. This is because, in this experiment, an equivalent shear beam (ESB) container was used to minimize the reflected wave of the container wall; however, the seismic interaction occurred in the low period because of the unfilled frame with soil on the top of the container (Fig. 1). This issue was detailed in a study by Lee *et al.* (2013) who designed an ESB container. However, excluding the short period range, a similar maximum response occurred around the period of 0.35 to 0.4 s in both the experimental and analysis models. The maximum responses for the experimental and analysis models subjected to the Gyeongju seismic motions were 0.55 and 0.6 g, respectively. Although there were some differences in response for the analysis models of the other six seismic motions, they all showed maximum responses around a period of 0.35 to 0.4 s. In conclusion, the analysis model appears to adequately simulate the depth-dependent PGA and acceleration amplification characteristics based on the period when compared with the experimental model.

3.2 Results of 1DSR analysis

Fig. 10 shows the results of the 1DSR analyses performed using the sand model derived by Darendeli (2001) and the rubble mound model derived by Lee *et al.* (2009). The analysis displays the results of a ground relative density of 55% and an input acceleration of 0.22 g. In each figure, the PGA by depth is compared between the CRM and NRM models. Based on the figures, all the PGAs were derived similarly at depths of 2 m or more, where a rubble mound was not installed. However, the PGA significantly decreased at the location where the rubble mound was installed. From the results of the seismic motions of Gyeongju in Fig. 10(a), 23% of the PGA decreased from the upper part of the ground because of the installation of the rubble mound, showing a decrease similar to that of the experimental model. Further, in the case of Figs. 10(b)-

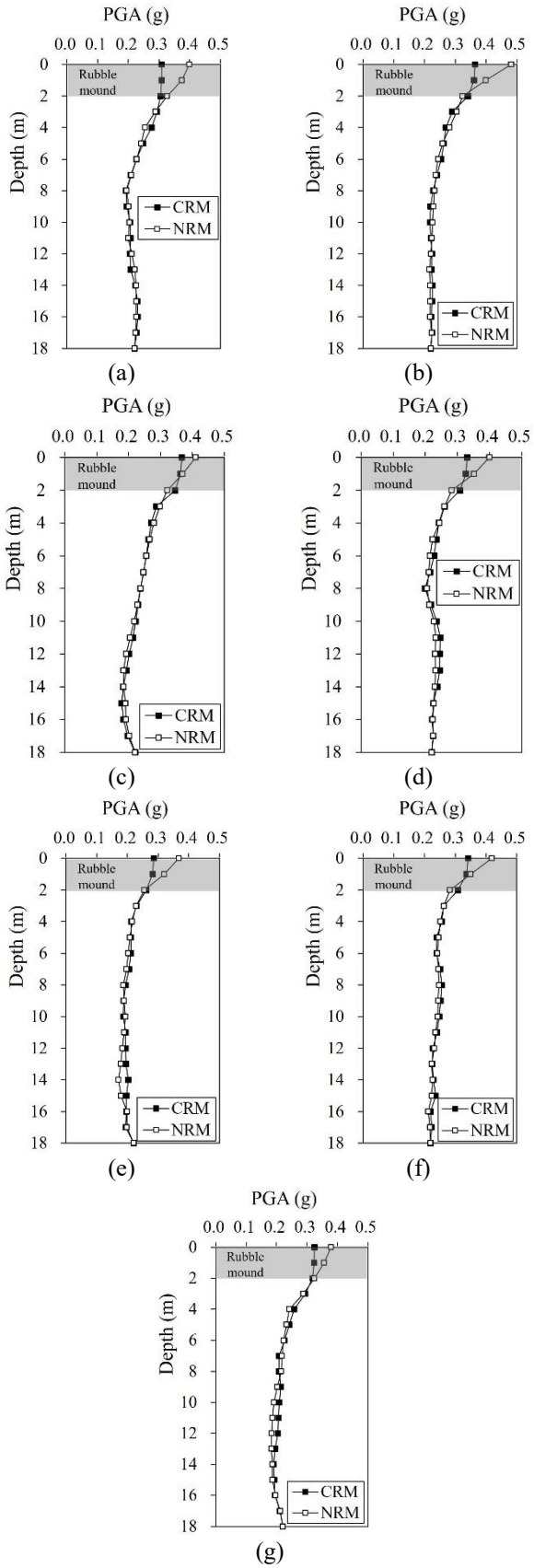

Fig. 10 PGA along the depth of NRM and CRM analysis models (relative density of 55%, input base acceleration: 0.22g): (a) Gyeongju, (b) Pohnag, (c) Borah, (d) Nahanni, (e) Romania, (f) Tabas-Dayhook and (g) Tabas-Tabas seismic motion (in prototype scale)

10(g), a difference of 11 to 24% occurred, indicating that the acceleration response decreased when the rubble mound was installed.

The decrease in acceleration response when rubble mound was installed can be explained by normalized shear modulus and damping ratio curve in Fig. 7. As seen in the figure, with increasing shear strain, the normalized shear modulus was higher and damping ratio was lower in the rubble mound model compared to the sand models. In the case of the rubble mound model, at a strain of 0.1%, the normalized shear modulus and damping ratio were founded to be 0.34 and 12.5, respectively, whereas in Darendeli (2001) sand model, they were founded to be 0.27 and 14.7, respectively. Consequently, the installation of the rubble mound results in an increase in shear resistance of ground and a decrease in soil deformation, leading to a reduced acceleration response in the upper part of ground.

Fig. 11 shows the PGA response of the ground surface of the analysis models based on the input accelerations. Figs. 11(a) and 11(b) show the results of the analysis model with ground relative densities of 55% and 80%, respectively. Each figure includes trend lines representing the average values of the NRM and CRM models. The solid black line represents the CRM results, and the dotted black line represents the NRM results. Based on the soil model with 55% relative density in Figure 11(a), as the input acceleration increases, the PGA increases linearly, and the difference in PGA between NRM and CRM models also increases. At 0.063 g, the difference in PGA was approximately 0.01 g; however, at 0.22 g, the difference increased to as much as 0.07 g. Contrarily, in the soil model with 80% relative density in Fig. 11(b), the PGA increased linearly as the input acceleration increased, however, the PGA difference between NRM and CRM models did not increase. The difference in input acceleration for both 0.063 and 0.22 g was derived to approximately 0.01 g.

Fig. 12 shows the acceleration amplification ratio (AAR) based on the results in Fig. 11 to analyze the difference in the PGA of the NRM and CRM models. The AAR was calculated by dividing the PGA of the CRM model by that of the NRM model. The figure includes trend lines representing the average value of the analysis models, with dashed lines indicating the results of 80% relative density and dotted lines indicating the results of 55% relative density. Additionally, the figure shows the AAR results obtained from the centrifuge model tests. As shown in the figure, most responses were derived at < 1. This is because the PGA is derived to be smaller when the rubble mound is installed because it restrains the deformation of the ground surface compared to the case where the rubble mound is not installed. In the analysis model with a relative density of 55%, AAR decreased significantly as the input acceleration increased. At 0.063 g, the AAR showed a decrease of approximately 8%, while at 0.22 g, it was approximately 18%. Similarly, for an experimental model with a relative density of 50%, a significant decrease in AAR with increasing input acceleration was observed, consistent with the analysis model. This suggests that the 1DSR analysis appropriately simulates the actual ground-acceleration amplification characteristics. However, for the analysis model with a relative density of 80%, the AAR decrease remained within 3%, regardless of increasing input

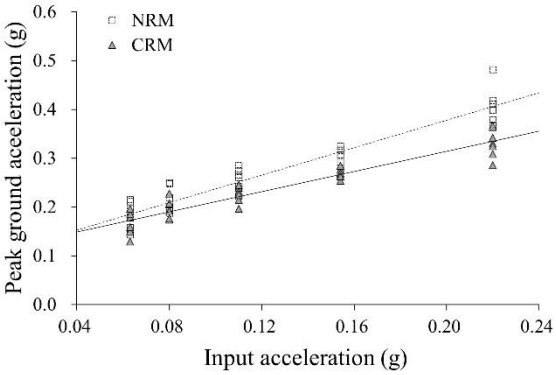

(a)

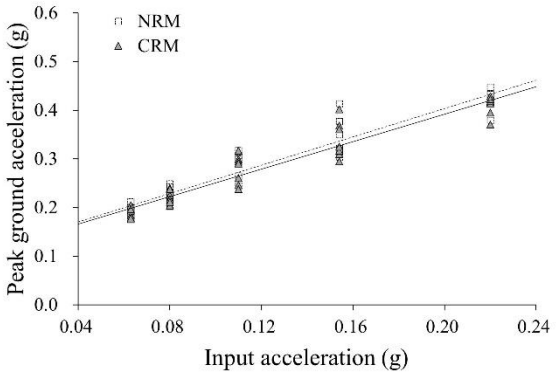

(b)

Fig. 11 PGA according to the input base acceleration of NRM and CRM model: (a) Relative density of 55% and (b) Relative density of 80% (in prototype scale)

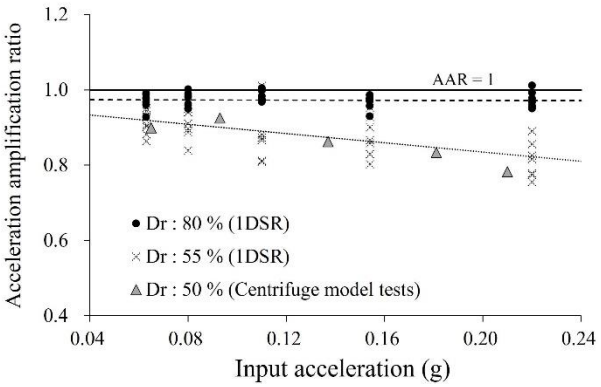

Fig. 12 AAR according to the input base acceleration of NRM and CRM model (in prototype scale)

acceleration. This is because, in dense ground, where ground deformation does not increase significantly with input acceleration, the differences with and without the rubble mound do not increase. Contrarily, in loose ground, where the ground deformation increases considerably with the input acceleration, the differences with and without the rubble mound also increase.

In Fig. 13, the response spectrum and AAR of the NRM and CRM analysis models are presented to analyze the frequency characteristics based on the installation of the rubble mound. The AAR is calculated by dividing the spectral acceleration of the CRM model by that of the NRM model. Figs. 13(a) and 13(b) show the acceleration of the

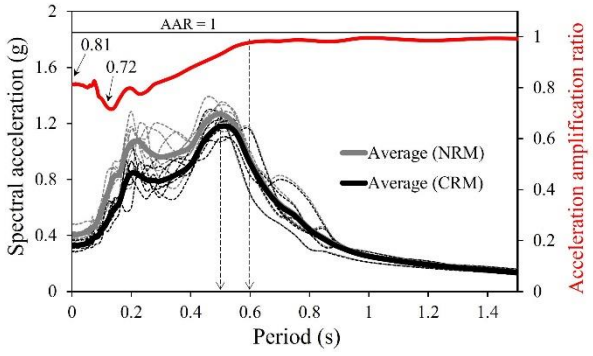

(a)

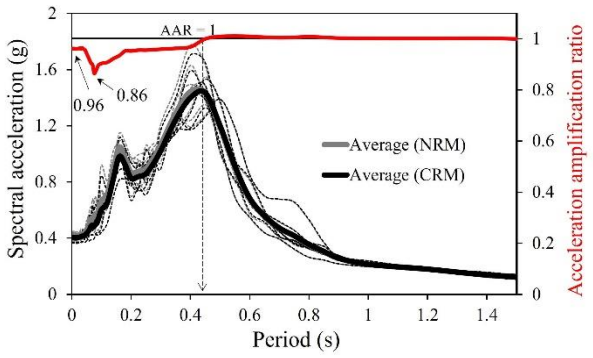

(b)

Fig. 13 Response spectrum and AAR of NRM and CRM models: (a) Relative density of 55% and (b) Relative density of 80% (in prototype scale)

ground surface with relative densities of 55 and 80%, respectively. The black and gray dotted lines in each figure represent the responses of the CRM and NRM models subjected to seven seismic motions, whereas the black and gray solid lines represent the average values of these responses. Comparing the relative densities of 55 and 80% models, the higher relative density models exhibited larger acceleration responses compared to lower relative density models. For the relative density of 55% model, the CRM and NRM yielded maximum responses of 1.18 and 1.27 g respectively. However, for the relative density of the 80% model, both the CRM and NRM showed a maximum response of 1.44 g. Additionally, the higher relative density models tended to have maximum responses closer to the short period range. In the case of the 55% model, the maximum response occurred at a period of 0.5 s, while for the relative density of the 80% model, it occurred at a period of 0.45 s. This can be attributed to the higher stiffness of the ground in the higher relative density model, which leads to a significant inclusion of the short period component. Next, a comparison of the AAR in Fig. 13 provides insights into the AAR based on the periods of seismic motion. For the 55% model, the AAR at period 0 s (PGA) and 0.14 s were calculated to be 0.81 and 0.72, respectively, with a decrease in response observed until 0.6 s. Conversely, for the relative density of the 80% model, the AAR at period 0 s (PGA) and 0.08 s were calculated to be 0.96 and 0.86, respectively, with a decrease in response until around 0.45 s. This indicates that the influence of the installation of the rubble mound was relatively small in the

higher relative density model, particularly in terms of the period-dependent response.

In conclusion, reinforcing the ground with rubble mound reduces the ground surface PGA and short period responses by approximately 28%, whereas it has minimal impact on long period response. Furthermore, it was observed that in the lower relative density ground, the decrease rate of the response and range of the decreasing periods were greater. Considering that the range of decreasing short period periods corresponds to the critical periods in the design response spectrum, the installation of a rubble mound can effectively decrease the acceleration response of the ground surface.

This study focused on analyzing the acceleration amplification characteristics of the ground by reinforcing a rubble mound. As a result, experiments were conducted on dry sand to mitigate the impact of water wave force and liquefaction. In the case of the 1DSR analysis, the impact of slopes was not taken into account, consequently neglecting the residual displacements attributed to lateral spreading.

The residual displacement can be dominated at long period component; therefore, this oversight could potentially result in differences in the long period responses. Additionally, deriving the properties near the slope surface is generally challenging. Hence, this study employed rubble mound properties from Lee *et al.* (2009) and sand properties from Darendeli (2001) for the analyses. It is recommended that future analyses and validations comprehensively address these aspects for a more thorough understanding.

4. Conclusions

In this study, the acceleration amplification characteristics of a rubble mound installed in an open-type wharf were investigated by analyzing the results of dynamic centrifuge model tests. Based on these results, 1DSR analyses were conducted. For the analyses, 140 model cases were considered, which encompassed two different relative soil densities, the presence or absence of a rubble mound, seven different input seismic motions, and five levels of acceleration amplitudes. Based on these parameters, analyses were conducted, and the amplification characteristics of the ground reinforced with rubble were analyzed using the obtained results. The following conclusions were drawn:

From the centrifuge model tests, when a 2 m thick rubble mound was installed on the ground surface of the embankment, the acceleration response decreased by approximately 22% and the ground subsidence decreased by approximately 50%. Moreover, the imbalance in subsidence between the lower and upper positions on the ground was significantly reduced by eight-fold to two-fold. Therefore, it can be inferred that installing a rubble mound on an embankment enhances the seismic performance in terms of both acceleration and displacement.

Based on the experimental results, 1DSR analyses were conducted using the sand model of Darendeli (2001) and the rubble mound model of Lee *et al*. (2009). The analysis aimed to compare the PGA and response spectra of the experimental and analytical models. Consequently, the analysis model appears to adequately simulate the depth-dependent PGA and acceleration amplification characteristics based on the period when compared to the experimental model.

The 1DSR analyses indicated that when the ground was reinforced with a rubble mound, the PGA of the ground surface decreased. In the 55 % relative density model, as the input acceleration increased, the PGA decreased significantly, ranging from 8 to 18 %. However, in the 80 % relative density model, the PGA decreased by 3%, regardless of the input acceleration. This is because, in dense ground, where ground deformation does not increase significantly with input acceleration, the differences with and without the rubble mound do not increase.

When the ground was reinforced with the rubble mound, the short period responses decreased, whereas the long period responses remained relatively unaffected. In the 55% relative density model, short period responses below 0.6 s decreased by approximately 28%, whereas in the case of the 80% relative density model, short period responses below 0.45 s decreased by approximately 14%. Considering that the range of decreasing short period periods corresponds to the critical periods in the design response spectrum, the installation of a rubble mound can effectively decrease the acceleration response of the ground surface.

Acknowledgments

This research was supported by the “Korea Institute of Marine Science & Technology Promotion (KIMST) (No. 2016-0065)” and by the “National Research Foundation of Korea (NRF) grant funded by the Korea government (MSIT) (No. 2022R1F1A1071805).

References

Al Atik, L. and Abrahamson, N. (2010), “An improved method for nonstationary spectral matching”, *Earthq. Spectra*, **26**(3), 601-617. https://doi.org/10.1193/1.3459159.

Balomenos, G.P. and Padgett, J.E. (2018), “Fragility analysis of pile-supported wharves and piers exposed to storm surge and waves”, *J. Wat., Port, Coast. Ocean Eng*., **144**(2), 04017046. https://doi.org/10.1061/(ASCE)WW.1943-5460.0000436.

Cihan, K. and Yuksel, Y. (2011), “Deformation of rubble-mound breakwaters under cyclic loads”, *Coast. Eng*., **58**(6), 528-539. https://doi.org/10.1016/j.coastaleng.2011.02.002.

Dammala, P.K., Krishna, A.M., Bhattacharya, S., Nikitas, G. and Rouholamin, M. (2017), “Dynamic soil properties for seismic ground response studies in Northeastern India”, *Soil Dyn. Earthq. Eng*., **100**, 357-370. https://doi.org/10.1016/j.soildyn.2017.06.003.

Darendeli, M.B. (2001), “Development of a new family of normalized modulus reduction and material damping curves”, Ph.D. Dissertation, University of Texas at Austin, Texas.

EduPro Civil Systems, Inc. (2017), ProShake: Ground response analysis program version 2.0, User’s manual.

Hudson, R.Y. (1959), “Laboratory investigation of rubble-mound breakwaters”, *J. Wat. Harb. Div*., **85**(3), 93-121. https://doi.org/10.1061/JWHEAU.0000142.

Lee, H.J., Locat, J., Desgagnés, P., Parsons, J.D., McAdoo, B.G.,

Orange, D.L., Puig, P., Wong, F.L., Dartnell, P. and Boulanger, E. (2007), "Submarine mass movements on continental margins", Continental margin sedimentation: from sediment transport to sequence stratigraphy, **37**, 213-274.

Lee, S.H., Kim, D.S., Choo, Y.W. and Choo, H.K. (2009), "Estimation of dynamic material properties for fill dam: II. Nonlinear Deformation Characteristics", *J. Kor. Geotech. Soc.*, **25**(12), 87-105 (in Korean).

Lee, S.H., Choo, Y.W. and Kim, D.S. (2013), "Performance of an equivalent shear beam (ESB) model container for dynamic geotechnical centrifuge tests", *Soil Dyn. Earthq. Eng.*, **44**, 102-114. https://doi.org/10.1016/j.soildyn.2012.09.008.

Lee, J.H., Ahn, J.K. and Park, D. (2015), "Prediction of seismic displacement of dry mountain slopes composed of a soft thin uniform layer", *Soil Dyn. Earthq. Eng.*, **79**, 5-16. https://doi.org/10.1016/j.soildyn.2015.08.008.

Lees, A.S. and Richards, D.J. (2011), "Centrifuge modelling of temporary roadway systems subject to rolling type loading", *Geomech. Eng.*, **3**(1), 45-59. https://doi.org/10.12989/gae.2011.3.1.045.

McCullough, N.J., Dickenson, S.E., Schlechter, S.M. and Boland, J.C. (2007), "Centrifuge seismic modeling of pile-supported wharves", *Geotech. Test. J.*, **30**(5), 349-359. https://doi.org/10.1520/GTJ14066.

Memos, C., Bouckovalas, G. and Tsiachris, A. (2001), "Stability of rubble-mound breakwaters under seismic action", *Coast. Eng.*, **2000**, 1585-1598. https://doi.org/10.1061/40549(276)123.

MOF. (Ministry of Oceans and Fisheries) (1999), Seismic design standards of harbour and port. Ministry of Oceans and Fisheries, Sejong, Korea (in Korean).

MOF. (Ministry of Oceans and Fisheries) (2017), Design standards of harbour and port. Ministry of Oceans and Fisheries, Sejong, Korea (in Korean).

MOIS. (Ministry of the Interior and Safety) (2017), Announcement of common application of seismic design criteria. Ministry of the Interior and Safety, Sejong, Korea (in Korean).

Najma, A. and Ghalandarzadeh, A. (2019), "Experimental study on the seismic behavior of composite breakwaters located on liquefiable seabed", *Ocean Eng.*, **186**, 106127. https://doi.org/10.1016/j.oceaneng.2019.106127.

PIANC. (International Navigation Association) (2001), Seismic design guidelines for port structures. International Navigation Association, Rotterdam, Netherlands.

Seed, H.B. and Idriss, I.B. (1970), "Soil moduli and damping factors for dynamic response analyses", Reoprt No. EERC 70; University of California, California, USA.

Su, L., Lu, J., Elgamal, A. and Arulmoli, A.K. (2017), "Seismic performance of a pile-supported wharf: Three-dimensional finite element simulation.", *Soil Dyn. Earthq. Eng.*, **95**, 167-179. https://doi.org/10.1016/j.soildyn.2017.01.009.

Vytiniotis, A., Panagiotidou, A.I. and Whittle, A.J. (2019), "Analysis of seismic damage mitigation for a pile-supported wharf structure", *Soil Dyn. Earthq. Eng.*, **119**, 21-35. https://doi.org/10.1016/j.soildyn.2018.12.020.

Ye, J. and Wang, G. (2015), "Seismic dynamics of offshore breakwater on liquefiable seabed foundation", *Soil Dyn. Earthq. Eng.*, **76**, 86-99. https://doi.org/10.1016/j.soildyn.2015.02.003

Ye, J.H. and Jeng, D.S. (2013), "Three-dimensional dynamic transient response of a poro-elastic unsaturated seabed and a rubble mound breakwater due to seismic loading", *Soil Dyn. Earthq. Eng.*, **44**, 14-26. https://doi.org/10.1016/j.soildyn.2012.08.011.

Yun, J., Han, J. and Kim, D. (2022), "Evaluation of seismic p-yp loops of pile-supported structures installed in saturated sand", *Geomech. Eng.*, **30**(6), 579-586. https://doi.org/10.12989/gae.2022.30.6.579.

Yun, J.W. and Han, J.T. (2023a), "Evaluation of the effect of rubble mound on pile through dynamic centrifuge model tests", *Geomech. Eng*, **33**(4), 415-425. https://doi.org/10.12989/gae.2023.33.4.415.

Yun, J.W. and Han, J.T. (2023b), "Evaluation of the dynamic bahavior of pile groups considering the kinematic force of the slope using centrifuge model tests", *Soil Dyn. Earthq. Eng.*, **173**, 108106. https://doi.org/10.1016/j.soildyn.2023.108106.

IC